IEEE Access
Multidisciplinary | Rapid Review | Open Access Journal

Received October 23, 2019, accepted November 8, 2019, date of publication November 18, 2019, date of current version December 2, 2019.

Digital Object Identifier 10.1109/ACCESS.2019.2953844

A Comparison of Surface-to-Coal Mine Roadway TEM and Surface TEM Responses to Water-Enriched Bodies

JIANGHAO CHANG[1,2], GUOQIANG XUE[1], AND REZA MALEKIAN[3], (Senior Member, IEEE)

[1]Key Laboratory of Mineral Resources, Institute of Geology and Geophysics, Chinese Academy of Sciences, Beijing 100029, China
[2]School of Exploration Technology and Engineering, Hebei GEO University, Shijiazhuang 050031, China
[3]Department of Electrical, Electronic and Computer Engineering, University of Pretoria, Pretoria 0002, South Africa

Corresponding author: Guoqiang Xue (ppxueguoqiang@163.com)

This work was supported in part by the National Key Research and Development Program of China under Grant 2017YFC0801405 and Grant 2018YFC0807804, in part by the Key Research and Development Program of Shaanxi Province under Grant 2017GY-175, and in part by the National Natural Science Foundation of China under Grant 51574250, Grant 41830101, Grant 41804073, and Grant 41674079.

ABSTRACT The surface transient electromagnetic method (TEM) is a geophysical technology normally used in detecting water-enriched zones. However, with an increase of mining depth, the accuracy and reliability of surface detection is gradually reduced, and surface TEM cannot meet the requirements of high-precision detection for coal mine production safety. In this study, surface-to-coal mine roadway TEM is proposed to detect water-enriched zones in coal mines. The resolution of this method in detecting targets, however, is still unknown. Based on a 1-D layered model, the surface-to-coal mine roadway TEM response is numerically simulated using the finite-difference time-domain method (FDTD). The results show that the surface-to-coal mine roadway TEM has higher resolution of the target above the underground receiving point and weaker resolution of the target below the receiving point. 3-D geo-electric models for typical water-enriched zones such as a water-filled mining goaf, a water-filled fault and a water-filled collapse column are established. The surface-to-coal mine roadway TEM responses are numerically simulated and compared with the surface TEM responses. The results show that for the goaf model, the surface-to-coal mine roadway TEM response is more sensitive than the surface TEM response. For fault and collapse column models, the surface-to-coal mine roadway response is more sensitive than surface response in the early delay stage but less sensitive in the late delay stage. The present study provides theoretical support for device selection and for data processing interpretation in actual work.

INDEX TERMS Transient electromagnetic method, borehole, surface-to-coal mine roadway, water-enriched zones, numerical modeling.

I. INTRODUCTION

The geological structures of coal mines have long spawned a series of environmental and security issues for the mining industry. Once filled with water, the goaf, collapse column and fault may also lead to water inrush in mines, thus affecting production safety [1]–[3]. Currently, effective prospecting of such water-enriched zones remains a difficult and unsettled issue. The geophysical technologies for coalfield exploration are applied either at the earth surface or in the underground mining roadways. Primary ground geophysical methods include the direct current electrical method, the transient electromagnetic method (TEM) and the controlled source audio-frequency magnetotelluric method.

TEM is a time-domain electromagnetic detection method based on the electromagnetic induction principle. It utilizes a nongrounded loop or grounded wire to transmit a stepped pulsed magnetic field into the earth. During the pause of the primary field, the time-varying changes of the induced secondary field in the underground media are measured to detect various geological targets in the ground [4]–[6]. TEM easily excites an induced current in a conductive layer, which makes it favorable for detecting water-filled structures [7]–[10].

The associate editor coordinating the review of this manuscript and approving it for publication was Mehmet Alper Uslu.

A normal survey of TEM for detecting water-enriched zones is conducted at the ground surface [11]–[13]. The resolution of TEM is related to the size of the transmitting loop, the transmitting loop current and the noise level, and it decreases with increasing depth. With an increase of mining depth, the geological conditions become more complex, and the depth of the target body gradually increases.

In recent years, underground TEM has been developed [14]–[17]. The transmitting and receiving loops for underground TEM are located within underground roadways that are closer to water-filled structures, resulting in higher detection accuracy. Moreover, it is easy to implement and can detect targets in different directions around the roadway. Nevertheless, due to the narrow space within roadways, only transmitting loops with side length of less than 3 m can be used. This greatly limits the detection depth of the method.

In view of the problems above, a surface-to-tunnel transient electromagnetic method is proposed to detect water-enriched zones in coal mines [18]. This method places a transmitting loop on the ground surface to excite an electromagnetic field in the earth, and the receiving loop is located in an underground roadway to observe the secondary field signal. This method takes account of both surface and underground TEM.

The response of surface to underground borehole TEM was tested three decades ago [19]. Eaton and Hohmann (1984) studied the borehole TEM responses of a thin horizontal conductor using a 2-D model [20]. West and Ward (1988) calculated the borehole TEM response of a three-dimensional fracture zone in a conductive half-space [21]. Meng and Pan (2012) studied the surface-hole TEM responses of a conductive plate and analyzed the effect of conductive overburden [22]. Wu *et al.* (2017) studied the approximate processing method of electric source borehole TEM and defined the full-field apparent resistivity [23]. Chen *et al.* (2019) analyzed the full-component response of electric source surface-to-borehole TEM [24].

In contrast to surface-to-borehole TEM, in surface-to-tunnel TEM the receiver can be moved along a coal mine tunnel. Since the hydrogeology of coal mines is complex, and water-enriched zones are diverse in both species and shapes, the resolution of surface-to-coal mine roadway TEM remains unclear. In response to these problems, in this study geoelectric models of such representative water-enriched zones as water-filled mining goafs, faults and collapse columns are established. The surface-to-coal mine roadway TEM responses are studied using the 3-D FDTD method and compared with the surface responses. The present study provides a basis for device selection and data processing interpretation in actual work.

II. SURFACE-TO-COAL MINE ROADWAY TEM

The surface-to-coal mine roadway TEM uses a large loop on the ground surface as a transmitting source and a small loop in an underground roadway as a receiver loop (as shown in Fig. 1). The transmitting current waveform of surface-to-coal mine roadway TEM is the same as that of surface TEM—a stepped current. During the pause of the primary field, the time-varying changes in the induced secondary field in underground media are measured by the receiver loop in the underground roadway. Through processing, analysis and interpretation of the induced secondary field information, various geological targets can be detected.

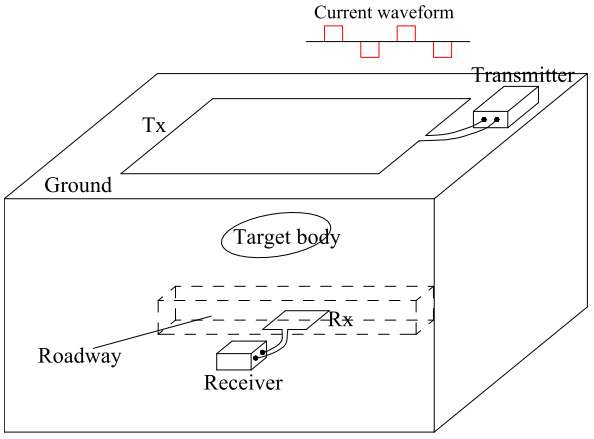

FIGURE 1. Schematic diagram of surface-to-coal mine roadway TEM.

III. 3-D FDTD FOR TRANSIENT ELECTROMAGNETIC FIELDS

For a homogeneous half-space, the surface magnetic field generated by the circular loop source in the frequency domain is given as [5]

$$H_z(\omega) = Ia \int_0^\infty \frac{\lambda^2}{\lambda + u} J_1(\lambda a)\, d\lambda, \tag{1}$$

where I is the intensity of the current in the transmitting loop, a is the radius of the transmitting loop, J_1 is the Bessel function of order one, and $u = \sqrt{\lambda^2 + k^2}$, where k is the wavenumber for the half-space. The receiving point is in the center of transmitting loop.

The underground magnetic field in the frequency domain is given as [5]

$$H_{1z}(\omega) = Ia \int_0^\infty \frac{\lambda^2}{\lambda + u} J_1(\lambda a)\, e^{-uz} d\lambda, \tag{2}$$

where z is the receiving depth.

For a transient electromagnetic field, the current waveform is a step wave:

$$I(t) = \begin{cases} I_0 & t < 0 \\ 0 & t > 0. \end{cases} \tag{3}$$

Using an inverse Fourier transform, the time derivative of the magnetic field can be calculated from [25]

$$\frac{dH(t)}{dt} = \frac{2}{\pi} \int_0^\infty Im[H(\omega)] \sin \omega t d\omega, \tag{4}$$

where $Im[H(\omega)]$ is the imaginary component of $H(\omega)$.

The above is the solution for a homogeneous half-space. When the underground medium is inhomogeneous, the numerical method should be used to solve it. The FDTD

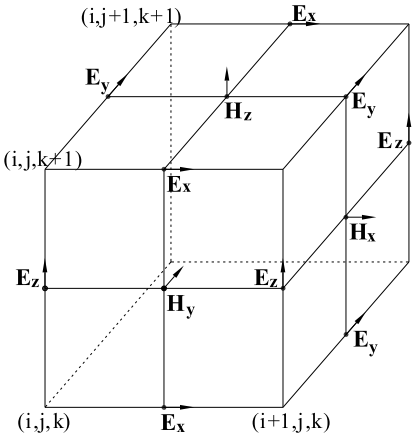

FIGURE 2. Field components in Yee grid [26].

method is the main method used in 3-D numerical simulation of transient electromagnetic fields. The grid used in FDTD is shown in Fig. 2 [26], which can naturally meet the continuity conditions of field components on a 3-D surface. In source-free regions, Maxwell's equations under quasi-static conditions are [27]

$$\nabla \times E = -\frac{\partial B}{\partial t}, \tag{5}$$

$$\nabla \times H = \sigma E + \gamma \frac{\partial E}{\partial t}, \tag{6}$$

$$\nabla \cdot B = 0, \tag{7}$$

$$\nabla \cdot J = 0, \tag{8}$$

where E is the electric field intensity, B is the magnetic induction intensity, H is the magnetic field intensity, σ is the conductivity of the medium, J is the conduction current density, and γ is the displacement permittivity. The introduction of displacement permittivity allows for less strict time-step requirements in the computation of the late-time electromagnetic field [27].

The equations above apply to the source-free regions. When applied in the source region, equation (6) should be modified [28], [29]:

$$\nabla \times H = \gamma \frac{\partial E}{\partial t} + \sigma E + J_s. \tag{9}$$

The iterative equations of electric and magnetic fields can be obtained by using discrete differencing for equations (5)–(9) [27].

The transient electromagnetic field can be simulated using the aforementioned methods in combination with an imposed convolutional perfectly matched layer [30] on underground boundaries.

IV. RESPONSE CHARACTERISTICS OF SURFACE-TO-COAL MINE ROADWAY TEM

A. COMPARISON OF SURFACE-TO-COAL MINE ROADWAY TEM AND SURFACE TEM RESPONSES

The receiving device of surface-to-coal mine roadway TEM is placed within the underground roadway, whereas that of conventional surface TEM is placed on the ground surface.

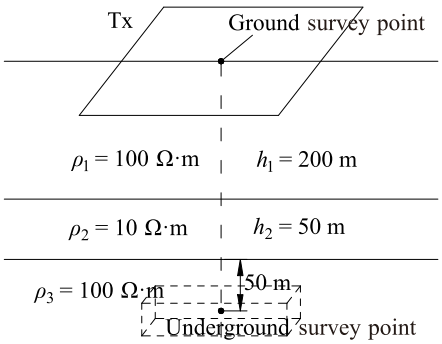

FIGURE 3. Comparison model of surface TEM and surface-to-coal mine roadway TEM responses.

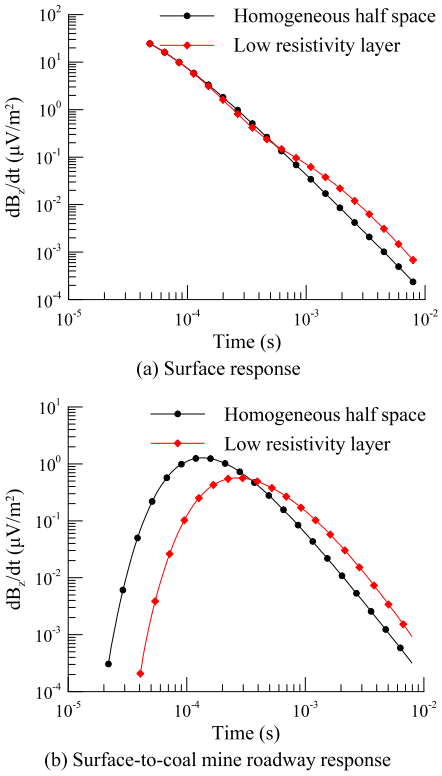

FIGURE 4. Response comparison of surface TEM and surface-to-coal mine roadway TEM.

To compare responses of the two methods to an abnormal underground body, a comparison model is established, as shown in Fig. 3. The background resistivity of the half-space is 100 Ω·m, and there is a 50 m-thick low-resistivity layer at 200 m depth that has a resistivity of 10 Ω·m. The size of the transmitting loop is 300 m × 300 m and the transmitting current wave is a trapezoidal wave. The mesh used in modeling is a non-uniform mesh. The grid near the transmitting loop is 10 m, and the grid becomes larger further from the transmitting loop. The surface receiving point is located at the center of the transmitting loop, and the roadway receiving point is located within the 300 m-deep roadway below the surface.

The comparative results are shown in Fig. 4. Fig. 4a is surface TEM response, and Fig 4b is surface-to-coal mine roadway response. As shown in Fig. 4a, the surface

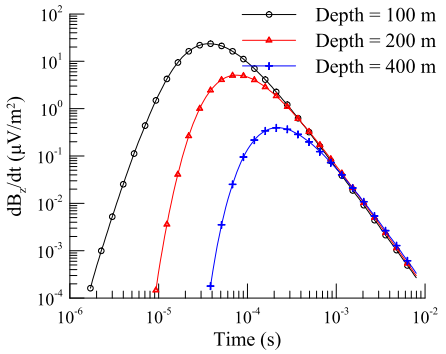

FIGURE 5. Surface-to-coal mine roadway TEM responses observed at varying depths.

response curve for the low-resistivity layer overlaps the background curve in the early delay stage. With time, the surface response curve for the low-resistivity layer diverges from the background curve. In the late delay stage, the low-resistivity layer response curve is higher than the background curve, reflecting the existence of underground low-resistivity layer. In Fig. 4b, the surface-to-coal mine roadway response strengthens over time in the early delay stage then weakens over time in the late delay stage. Here, the response curve under the influence of the low-resistivity layer is separated from the background curve in all time periods. The response curve under the influence of low-resistivity layer is lower than the background curve in the early delay stage but higher than the background curve in the late delay stage. Compared with the surface TEM response, the surface-to-coal mine roadway TEM response can reflect the low-resistivity layer over all time periods, while the surface response can achieve this only in the late delay stage, which shows that the surface-to-coal mine roadway response is more sensitive in distinguishing the underground abnormal body.

B. COMPARISON OF UNDERGROUND RESPONSES AT VARYING DEPTHS

To study the effect of receiving depth on underground response, a homogeneous half-space model is established. In the model, the resistivity is 100 Ω·m, and the transmitting loop is 300 m × 300 m in size. The receiving points are located right below the central point of transmitting loop at the depths of 100 m, 200 m and 400 m. The transient electromagnetic response is shown in Fig. 5, from which it can be seen that the responses observed at varying depths are composed of two stages: an ascending stage and a descending stage. The response strengthens with time in the early delay stage and weakens with time in the late delay stage. The response curve tends to be higher and attains the peak earlier at shallower receiving points. In the late delay stage, as time elapses, the response curves resulting from observation at different depths gradually overlap each other.

C. EFFECT OF RESISTIVITY OF ROOF AND FLOOR ROCKS ON SURFACE-TO-COAL MINE ROADWAY TEM RESPONSE

The receiving device of the surface-to-coal mine roadway TEM is placed within the underground roadway, so the

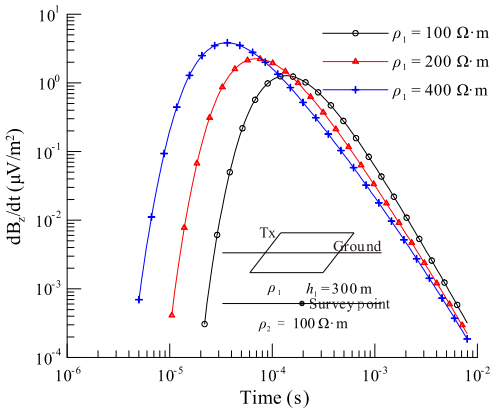

FIGURE 6. Surface-to-coal mine roadway TEM response for different resistivities of roof layer.

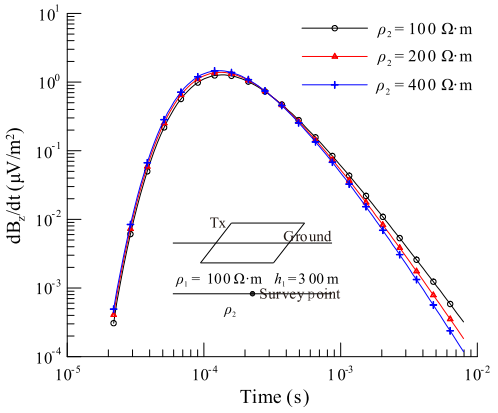

FIGURE 7. Surface-to-coal mine roadway TEM response for different resistivities of floor layer.

electrical properties of roof and floor rocks will affect the response. Fig. 6 shows the surface-to-coal mine roadway TEM response for different resistivities of roof layer. The transmitting loop is 300 m × 300 m in size, and the observation point is located 300 m below the ground. The resistivity of the roof layer ρ_1 is 100 Ω·m, 200 Ω·m and 400 Ω·m, and the resistivity of floor layer ρ_2 is 100 Ω·m. As shown in Fig. 6, the resistivity of roof layer can produce material effects on surface-to-coal mine roadway TEM response. A higher roof layer resistivity produces a higher response curve in the early delay stage, a lower response curve in the late delay stage, and a higher peak of the response curve.

By contrast, Fig. 7 shows the surface-to-coal mine roadway TEM response for different resistivities of the floor layer. The resistivity of the roof layer ρ_1 is 100 Ω·m, while three resistivities are given for the floor layer ρ_2: 100 Ω·m, 200 Ω·m and 400 Ω·m. As shown in Fig. 7, the response in the early delay stage is less affected by the floor layer resistivity than it had been by the roof layer resistivity. Instead, the response curve is affected by the floor layer only in the late stage. Comparing the responses of roof and floor, the roof layer has a greater effect on the response curve.

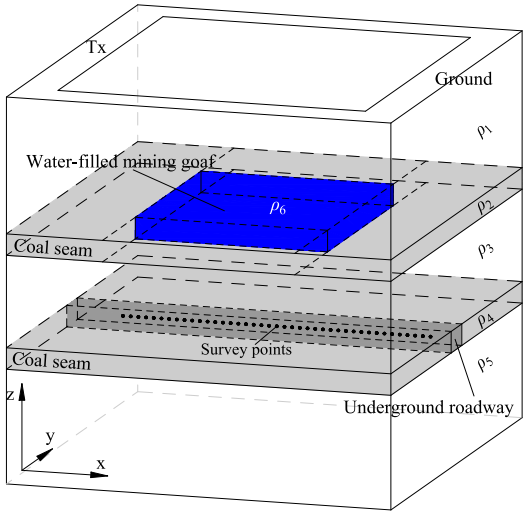

FIGURE 8. Geophysical model of water-filled mining goaf.

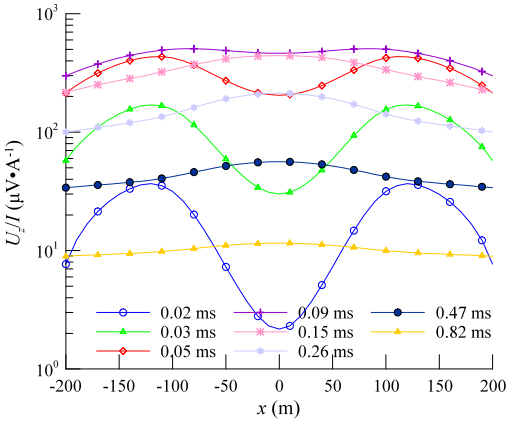

FIGURE 9. Surface-to-coal mine roadway TEM response of water-filled mining goaf.

V. SURFACE-TO-COAL MINE ROADWAY TEM RESPONSES OF WATER-ENRICHED ZONES IN COAL MINES

A. SURFACE-TO-COAL MINE ROADWAY TEM RESPONSE OF WATER-FILLED MINING GOAF

Fig. 8 shows a half-space geoelectric model established based on coalfield geological data. The water-filled mining goaf is 240 m below the ground, with a size of 200 m × 300 m × 10 m. The coal face is located 50 m below the floor of the goaf, and the coal seam is 10 m thick. The resistivity parameters in the model are as follows: $\rho_1 = 200\ \Omega\cdot$m, $\rho_2 = 800\ \Omega\cdot$m, $\rho_3 = 200\ \Omega\cdot$m, $\rho_4 = 800\ \Omega\cdot$m, $\rho_5 = 400\ \Omega\cdot$m and $\rho_6 = 5\ \Omega\cdot$m. The ground transmitting loop is 400 m × 400 m in size, and the receiving points are located within the roadway below the goaf. The equivalent area of the receiving loop is 200 m^2.

Fig. 9 shows the surface-to-coal mine roadway TEM response, in which the horizontal coordinates correspond to the survey points within the roadway, while the vertical coordinates represent the induced potential. The induced potential

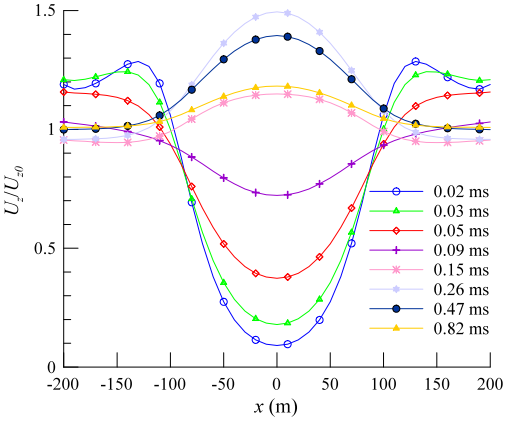

FIGURE 10. Relative induced potential of surface-to-coal mine roadway TEM response of water-filled mining goaf.

rises over time in the early delay stage (before 0.09 ms) and reaches a peak at 0.09 ms before declining. A comparison of response curves at different moments reveals the induced potential response increases gradually in the early delay stage, and the response curves are M-shaped, with the middle and two sides relatively lower due to the influence of the water-filled mining goaf and the offsets of survey points. In the late delay stage (after 0.15 ms), the induced potential decreases gradually, and the response curves are higher in the middle and lower on both sides. This is because a low-resistance body may hinder the change of the electromagnetic field and alleviate the attenuation of induced potential, so the induced potential around a water-filled goaf is higher in the late delay stage.

The observed induced potential is affected by the background field and the offset of survey points. The relative value of the induced potential can be obtained by normalizing the observed induced potential and the background value, as shown in Fig. 10. The horizontal coordinates correspond to the survey points within the roadway, while the vertical coordinates represent the relative induced potential U_z/U_{z0}, where U_z is the total induced potential response (induced potential in Fig. 9), and U_{z0} is the response of the normal coal seam without a water-filled goaf. The relative induced potential reflects the anomalous fields caused by the water-filled goaf. In Fig. 10, in the early delay stage (before 0.09 ms), the relative induced potential curve around the water-filled goaf (range: x = −100 m to x = 100 m) remains low, and the maximum difference between it and the background value is as high as 90%. In the late delay stage (after 0.15 ms), the relative induced potential curve around the water-filled goaf (range: x = −100 m to x = 100 m) is higher, and its maximum difference from the background value is 49%.

When the underground receiving point is transferred to the ground with the horizontal location unchanged, the surface TEM response can be observed. The response result is shown in Fig. 11, in which the horizontal coordinates correspond to the survey points on the ground surface, while the vertical coordinates represent the relative induced potential. According to Fig. 11, in the early delay stage (before 0.15 ms),

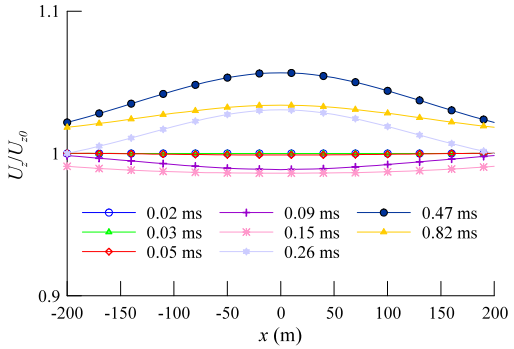

FIGURE 11. Relative induced potential of surface TEM response of water-filled mining goaf.

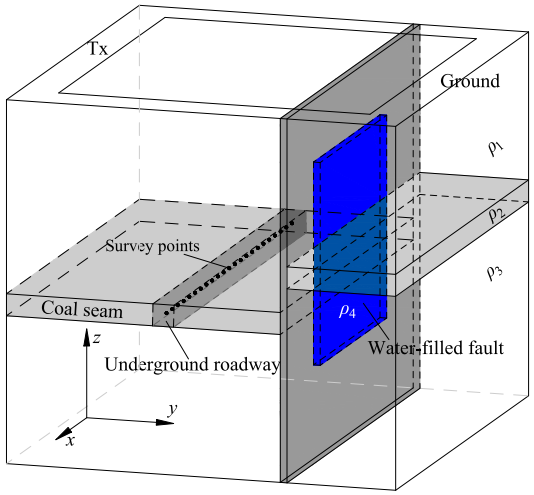

FIGURE 12. Geophysical model of water-filled fault.

the induced potential remains almost the same as the background value, suggesting the difference between the total response and the background field is insignificant during this period. When it comes to the late delay stage (after 0.26 ms), relative induced potential is much higher, and its maximum difference from the background value is 5.7%. When underground and ground responses are compared, the difference between the underground response and the background field is more significant, which proves the underground response is more sensitive in reflecting the water-filled goaf.

B. SURFACE-TO-COAL MINE ROADWAY TEM RESPONSE OF WATER-FILLED FAULT

Fig. 12 is a model of a water-filled fault, in which the coal seam where the underground roadway is located is 300 m below the ground with a thickness of 10 m. The water-filled fault exists 50 m away from the roadway. The throw of the fault is 20 m. The water-bearing zone in the fault is 200 m × 10 m × 300 m in size, and its central point is 200 m deep. The resistivity parameters of the model are as follows: $\rho_1 = 200\ \Omega\cdot$m, $\rho_2 = 800\ \Omega\cdot$m, $\rho_3 = 400\ \Omega\cdot$m and $\rho_4 = 5\ \Omega\cdot$m. The ground transmitting loop is 400 m × 400 m in size, receiving points are located within the underground roadway, and the equivalent area of the receiving loop is 200 m^2.

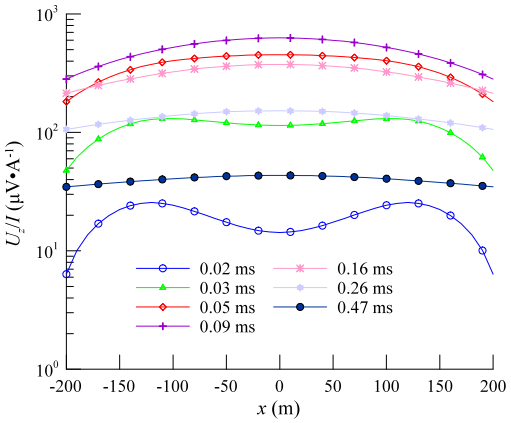

FIGURE 13. Surface-to-coal mine roadway TEM response of water-filled fault.

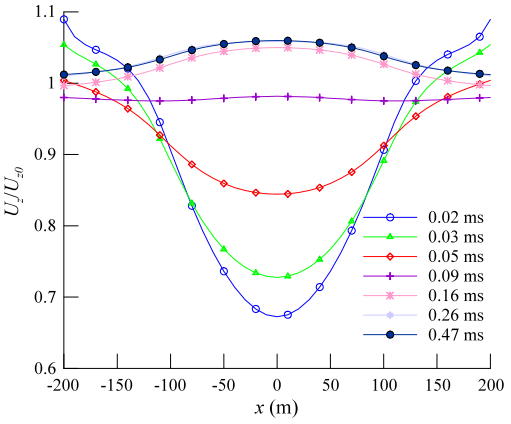

FIGURE 14. Relative induced potential of surface-to-coal mine roadway TEM response of water-filled fault.

Fig. 13 shows the surface-to-coal mine roadway TEM response, in which the horizontal coordinates correspond to the survey points within the roadway, while the vertical coordinates represent the induced potential. In the early delay stage (before 0.09 ms), the induced potential increases gradually. In the late delay stage (after 0.16 ms), the induced potential decreases gradually over time.

The induced potential in Fig. 13 is the total response under the effect of both normal strata and abnormal body, and it is affected by the offset of the survey points. The relative induced potential can be obtained by normalizing the observed induced potential and the background value, which can reflect the response of an abnormal body, as shown in Fig. 14. In the figure, U_z is total induced potential response (induced potential in Fig. 13), and U_{z0} is the response without water in the fault. In Fig. 14, in the early delay stage (before 0.09 ms), the relative induced potential curve around the water-filled fault (range: x = −100 m to x = 100 m) is lower, and its greatest difference from the background value reaches 33%. In the late delay stage (after 0.16 ms), the relative induced potential around the water-filled fault is higher, while this period witnesses an attenuation of the

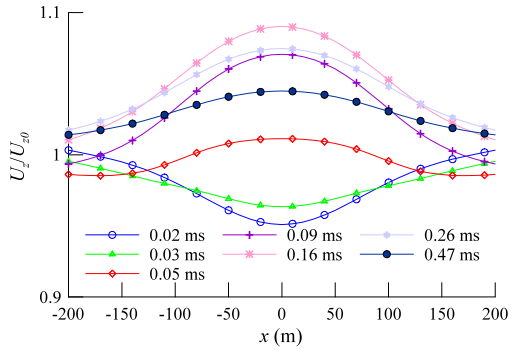

FIGURE 15. Relative induced potential of surface TEM response of water-filled fault.

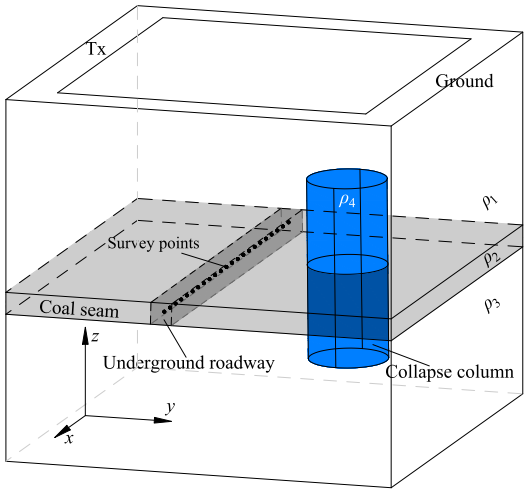

FIGURE 16. Geophysical model of water-filled collapse column.

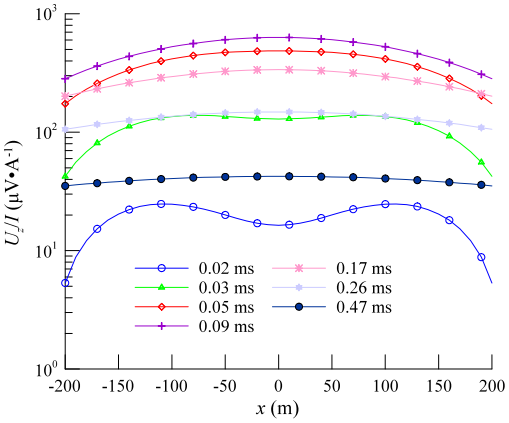

FIGURE 17. Surface-to-coal mine roadway TEM response of water-filled collapse column.

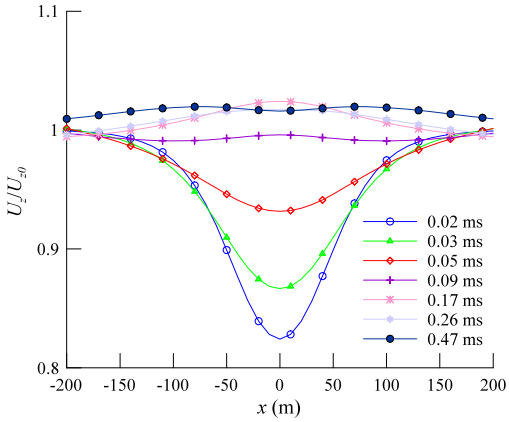

FIGURE 18. Relative induced potential of surface-to-coal mine roadway TEM response of water-filled collapse column.

induced potential. This attests that the water-filled zone may alleviate the attenuation of the induced potential.

When the underground receiving point is transferred to the ground with the horizontal location unchanged, the surface TEM response can be observed. The response result is shown in Fig. 15, in which the horizontal coordinates correspond to the survey points on ground surface, while the vertical coordinates represent the relative induced potential. According to Fig. 15, the surface response follows rules similar to those for the underground response, for both response curves remain lower in the early delay stage but move higher in the late delay stage. However, the surface response tends to show a greater difference from the background field in the late delay stage, as the most significant difference reaches 9%. A comparison of the underground response with ground response reveals the former is more sensitive in reflecting the water-filled fault in the early stage, while the ground response excels in the late delay stage.

C. SURFACE-TO-COAL MINE ROADWAY TEM RESPONSE OF WATER-FILLED COLLAPSE COLUMN

Fig. 16 is a model of water-filled collapse column. The coal seam where the underground roadway is located is 300 m below the ground surface and has a thickness of 10 m. The water-filled collapse column is on the lateral wall of the roadway. Its axis is 100 m away from the roadway, and the radius is 50 m. The top of the collapse column is 50 m underground, and its height is 300 m. The resistivity parameters of the model are as follows: $\rho_1 = 200\ \Omega\cdot$m, $\rho_2 = 800\ \Omega\cdot$m, $\rho_3 = 400\ \Omega\cdot$m and $\rho_4 = 5\ \Omega\cdot$m. The ground transmitting loop is 400 m × 400 m in size, the receiving points are located within the underground roadway, and the equivalent area of the receiving loop is 200 m^2.

Fig. 17 shows the surface-to-coal mine roadway TEM response, in which the horizontal coordinates correspond to the survey points within the roadway, while the vertical coordinates represent the induced potential. In the early delay stage (before 0.09 ms), the induced potential increases gradually. In the late delay stage (after 0.17 ms), the induced potential decreases gradually over time.

The observed induced potential is affected by the background field and the offset of survey points. The relative value of the induced potential can be obtained by normalizing the observed induced potential and the background value, as shown in Fig. 18. The horizontal coordinates correspond

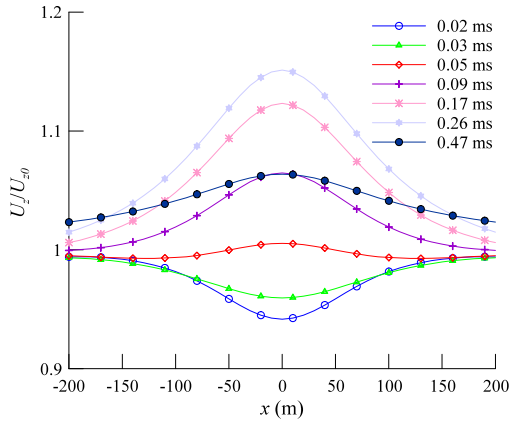

FIGURE 19. Relative induced potential of surface TEM response of water-filled collapse column.

to the survey points within the roadway, while the vertical coordinates represent the relative induced potential U_z/U_{z0}, where U_z is the total induced potential response (induced potential in Fig. 17), and U_{z0} is the response of the normal coal seam without the water-filled collapse column. In Fig. 18, in the early delay stage (before 0.09 ms), the relative induced potential around the collapse column is lower, while in the late delay stage (after 0.17 ms), the induced potential is almost the same as the background value, indicating there are insignificant differences between the response and the background field under the influence of the collapse column during this period of time.

When the underground receiving point is transferred to the ground with the horizontal location unchanged, the surface TEM response can be observed. The response result is shown in Fig. 19, in which the horizontal coordinates correspond to the survey points on the ground surface, while the vertical coordinates represent the relative induced potential. According to Fig. 19, the surface response follows rules similar to those for the underground response, for the induced potential around the collapse column remains low in the early delay stage. In the late delay stage, it is much higher and significantly different from the background field. In accordance with a comparison of underground and surface responses, in the early delay stage, the underground response is more sensitive in reflecting the collapse column, while surface response outperforms the underground in the late delay stage.

VI. CONCLUSION

Surface-to-coal mine roadway TEM is a novel working form developed from surface TEM for detecting water-enriched zones. Geoelectric models of some typical water-enriched zones such as water-filled goafs, faults and collapse columns are established. The surface-to-coal mine roadway TEM response is studied using the 3-D FDTD method, and a comparative analysis is made with surface TEM response. The conclusions are as follows:

(1) For a 1-D layered medium, resistivity of the rock layer above the receiving point can significantly affect the surface-to-coal mine roadway TEM response, while the rock layer below the receiving point affects the response curve in a less significant way. This indicates higher resolution of the surface-to-coal mine roadway TEM in distinguishing targets above the receiving point.

(2) Compared with surface TEM response, the surface-to-coal mine roadway response reflects the goaf more clearly, which indicates that the surface-to-coal mine roadway TEM is more sensitive to the resolution of the goaf.

(3) For fault and collapse column models, the surface-to-coal mine roadway TEM response is more sensitive in the early delay stage but less sensitive than surface response in the late delay stage. This shows that the surface TEM and the surface-to-coal mine roadway TEM may be combined in detecting faults and collapse columns, so as to embrace the strengths of the two methods at the same time.

DECLARATION OF INTEREST

The authors declare that there is no conflict of interests regarding the publication of this paper.

REFERENCES

[1] Q. Wu, Y. Liu, L. Luo, S. Liu, W. Sun, and Y. Zeng, "Quantitative evaluation and prediction of water inrush vulnerability from aquifers overlying coal seams in Donghuantuo Coal Mine, China," *Environ. Earth Sci.*, vol. 74, no. 2, pp. 1429–1437, 2015.

[2] J.-H. Chang, J.-C. Yu, and Z.-X. Liu, "Three-dimensional numerical modeling of full-space transient electromagnetic responses of water in goaf," *Appl. Geophys.*, vol. 13, no. 3, pp. 539–552, 2016.

[3] Q. Liu, Y. Sun, Z. Xu, S. Jiang, P. Zhang, and B. Yang, "Assessment of abandoned coal mines as urban reservoirs," *Mine Water Environ.*, vol. 38, no. 2, pp. 215–225, 2019.

[4] A. A. Kaufman and G. V. Keller, *Frequency and Transient Soundings*. New York, NY, USA: Elsevier, 1983.

[5] M. N. Nabighian, *Electromagnetic Methods in Applied Geophysics: Theory*, vol. 1. Tulsa, OK, USA: Society of Exploration Geophysicists, 1988.

[6] H. R. Piao, *Theory of Electromagnetic Sounding*. Beijing, China: Geological Publishing House (in Chinese), 1990.

[7] G. Xue, W. Chen, and S. Yan, "Research study on the short offset time-domain electromagnetic method for deep exploration," *J. Appl. Geophys.*, vol. 155, pp. 131–137, Aug. 2018.

[8] G. Xue, D. Hou, and W. Qiu, "Identification of double-layered water-filled zones using TEM: A case study in China," *J. Environ. Eng. Geophys.*, vol. 23, no. 3, pp. 297–304, 2018.

[9] G.-Q. Xue, W. Chen, Z.-J. Ma, and D.-Y. Hou, "Identifying deep saturated coal bed zones in china through the use of large loop TEM," *J. Environ. Eng. Geophys.*, vol. 23, no. 1, pp. 135–142, 2018.

[10] G.-Q. Xue, K. Chen, W.-Y. Chen, and Z. Tian, "The determination of the burial depth of coal measure strata using electromagnetic data," *J. Environ. Eng. Geophys.*, vol. 23, no. 1, pp. 125–134, 2018.

[11] S. Yan, G.-Q. Xue, W.-Z. Qiu, H. Li, and H.-S. Zhong, "Feasibility of central loop TEM method for prospecting multilayer water-filled goaf," *Appl. Geophys.*, vol. 13, no. 4, pp. 587–597, 2016.

[12] G. Q. Xue, J. L. Cheng, N. N. Zhou, W. Y. Chen, and H. Li "Detection and monitoring of water-filled voids using transient electromagnetic method: A case study in Shanxi, China," *Environ. Earth Sci.*, vol. 70, no. 5, pp. 2263–2270, 2013.

[13] W. Chen, G. Xue, A. L. Olatayo, K. Chen, M. Y. Khan, W. Chen, L. Zhang, and W. Chen, "A comparison of loop time-domain electromagnetic and short-offset transient electromagnetic methods for mapping water-enriched zones—A case history in Shaanxi, China," *Geophysics*, vol. 82, no. 6, pp. B201–B208, 2017.

[14] J. C. Yu, Z. X. Liu, S.-C. Liu, and J.-Y. Tang, "Theoretical analysis of mine transient electromagnetic method and its application in detecting water burst structures in deep coal stope," *J. China Coal Soc.*, vol. 32, no. 8, pp. 818–821, 2007.

[15] J. Cheng, F. Li, S. Peng, X. Sun, J. Zheng, and J. Jia, "Joint inversion of TEM and DC in roadway advanced detection based on particle swarm optimization," *J. Appl. Geophys.*, vol. 123, pp. 30–35, Dec. 2015.
[16] J. Chang, B. Su, R. Malekian, and X. Xing, "Detection of water-filled mining goaf using mining transient electromagnetic method," *IEEE Trans. Ind. Informat.*, to be published.
[17] J. Chang, J. Yu, J. Li, G. Xue, R. Malekian, and B. Su, "Diffusion law of whole-space transient electromagnetic field generated by the underground magnetic source and its application," *IEEE Access*, vol. 7, pp. 63415–63425, 2019.
[18] Z. Jiang, L. Liu, S. Liu, and J. Yue, "Surface-to-underground transient electromagnetic detection of water-bearing goaves," *IEEE Trans. Geosci. Remote Sens.*, vol. 57, no. 8, pp. 5303–5318, Aug. 2019.
[19] A. V. Dyck and G. F. West, "The role of simple computer models in interpretations of wide-band, drill-hole electromagnetic surveys in mineral exploration," *Geophysics*, vol. 49, no. 7, pp. 957–980, 1984.
[20] P. A. Eaton and G. W. Hohmann, "The influence of a conductive host on two-dimensional borehole transient electromagnetic responses," *Geophysics*, vol. 49, no. 7, pp. 861–869, 1984.
[21] R. C. West and S. H. Ward, "The borehole transient electromagnetic response of a three-dimensional fracture zone in a conductive half-space," *Geophysics*, vol. 53, no. 11, pp. 1469–1478, 1988.
[22] Q. X. Meng and H. P. Pan, "Numerical simulation analysis of surface-hole TEM responses," (in Chinese), *Chin. J. Geophys.*, vol. 55, no. 3, pp. 1046–1053, Apr. 2012.
[23] J. Wu, X. Li, Q. Zhi, X. Deng, and J. Guo, "Full field apparent resistivity definition of borehole TEM with electric source," (in Chinese), *Chin. J. Geophys.*, vol. 60, no. 4, pp. 1595–1605, Apr. 2017.
[24] W. Y. Chen, S. X. Han, and G. Q. Xue, "Analysis on the full-component response and detectability of electric source surface-to-borehole TEM method," (in Chinese), *Chin. J. Geophys.*, vol. 62, no. 5, pp. 1969–1980, 2019.
[25] G. A. Newman, G. W. Hohmann, and W. L. Anderson, "Transient electromagnetic response of a three-dimensional body in a layered earth," *Geophysics*, vol. 51, no. 8, pp. 1608–1627, Aug. 1986.
[26] K. Yee, "Numerical solution of initial boundary value problems involving Maxwell's equations in isotropic media," *IEEE Trans. Antennas Propag.*, vol. 14, no. 3, pp. 302–307, May 1966.
[27] T. Wang and G. W. Hohmann, "A finite-difference, time-domain solution for three-dimensional electromagnetic modeling," *Geophysics*, vol. 58, no. 6, pp. 797–809, 1993.
[28] H. F. Sun, X. Li, and S. C. Li, "Three-dimensional FDTD modeling of TEM excited by a loop source considering ramp time," (in Chinese), *Chin. J. Geophys.*, vol. 56, no. 3, pp. 1049–1064, 2013.
[29] S. Li, H. Sun, X. Lu, and X. Li, "Three-dimensional modeling of transient electromagnetic responses of water-bearing structures in front of a tunnel face," *J. Environ. Eng. Geophys.*, vol. 19, no. 1, pp. 13–32, 2014.
[30] J. A. Roden and S. D. Gedney, "Convolution PML (CPML): An efficient FDTD implementation of the CFS–PML for arbitrary media," *Microw. Opt. Technol. Lett.*, vol. 27, no. 5, pp. 334–339, 2000.

JIANGHAO CHANG received the Ph.D. degree in geophysics from the China University of Mining and Technology, Xuzhou, China, in 2017. He was a Lecturer with Hebei GEO University, Shijiazhuang, China, in 2017. He is currently a Postdoctoral Researcher with the Key Laboratory of Mineral Resources, Institute of Geology and Geophysics, Chinese Academy of Sciences. His research interest includes electromagnetic prospecting.

GUOQIANG XUE is currently a Researcher with the CAS Key Laboratory of Mineral Resources, with an emphasis in transient electromagnetic exploration and applications. His researches focus on TEM pseudo-seismic interpretation methods, TEM tunnel predication studies, large loop TEM exploration technology, the TEM response of short-offset excited by grounded electric sources, and the analysis of time-varying point charge infinitesimal assumptions in the TEM field.

REZA MALEKIAN (M'10–SM'17) is currently an Extraordinary Professor with the Department of Electrical, Electronic and Computer Engineering and the Past Head of the Advanced Sensor Networks Research Group, University of Pretoria. He is also a Chartered Engineer. His research focuses on advanced sensor networks and technologies. He is a Professional Member of the British Computer Society and an Associate Editor of the IEEE INTERNET OF THINGS and the IEEE TRANSACTIONS ON INTELLIGENT TRANSPORTATION SYSTEMS.